

Ultrasonic measurements of the elastic stiffness constants of oriented polyethylene*

J. G. Rider and K. M. Watkinson†

Department of Physics, University of Surrey, Guildford, Surrey, UK

(Received 22 December 1977)

High density polyethylene (Rigidex 9), a high density copolymer of polyethylene and poly(butene-1) (Rigidex 2000), and low density polyethylene (Alkathene WJG 11) were oriented by hot drawing. The crystalline texture, as determined by wide- and low-angle X-ray diffraction, was a highly oriented chain axis in the draw direction with random orientation transversely and with lamellae surfaces perpendicular to the draw direction. Elastic stiffness constants were measured by a contact-probe ultrasonic pulse technique at 2.5 MHz both before and after annealing in a temperature range which did not significantly alter the crystalline texture. Assuming orthorhombic symmetry the nine stiffness constants of Rigidex 2000 and the three longitudinal and three shear stiffness constants of Rigidex 9 were measured after drawing and after subsequent annealing. Only the longitudinal constants of Alkathene were measured, as shear waves could not be transmitted. The longitudinal stiffness in the draw direction was markedly affected by drawing and by annealing, while the crystalline texture remained substantially unchanged; by comparison the other stiffness constants showed little change. Drawn Rigidex 9 reached a tensile modulus in the draw direction of 69 GPa. The results are compared with 'static' and low frequency measurements reported in the literature.

INTRODUCTION

Interest in the mechanical properties of oriented polyethylene has increased recently with the discovery that high values of tensile modulus can be produced in this material. Formal and structural models of draw-oriented polyethylene have been suggested and the source of the high modulus discussed¹⁻⁸.

The present paper gives the results of measuring, at room temperature, the elastic stiffness constants of draw-oriented polyethylene by means of an ultrasonic pulse technique at a frequency of 2.5 MHz. Two types of high density linear polyethylene and one type of low density branched polyethylene were investigated. All three had a similar crystalline texture; high moduli were obtained with the two high density types. The effect of annealing was studied over a range of temperatures which did not significantly change the crystalline texture as revealed by wide- and low-angle X-ray diffraction but which did substantially reduce the stiffness in the orientation direction.

The velocities of longitudinal and shear ultrasonic stress pulses of MHz frequency have been measured in unoriented polyethylene⁹⁻¹¹. From these results we have calculated the corresponding longitudinal and shear stiffness constants and compare them with our own measurements given here.

Ultrasonic techniques have also been used for determining the stiffness constants of oriented thermoplastic amorphous polymers^{12,13}, and of fibre reinforced materials^{14,15}, but not apparently, of oriented polyethylene. The authors cited in refs 12 to 15 used liquid immersion techniques with varying angle of incidence; the measuring procedure and reduction

of data formed a comparatively lengthy process. Using contact probes on suitably cut test pieces, as we did, the measurement of all nine elastic constants of a material of orthorhombic symmetry is quick and simple.

The five elastic compliance constants of oriented and transversely isotropic polyethylene fibres have been measured at room temperature¹⁶ using 'static' (1 min modulus) and low frequency (torsion pendulum) methods. Buckley¹⁷ has given graphs of the compliance constants s_{22} and s_{23} , and the combination $s_{44} + 2s_{23}$, measured (after 10 sec creep) on oriented polyethylene sheet in the temperature range -183° to -70° C. A comparison of these results with our own is attempted in the discussion section of the present paper.

EXPERIMENTAL

Preparation of material

Two linear polyethylenes, Rigidex 9 and Rigidex 2000, and a branched polyethylene, Alkathene WJG 11, were used in this work. Rigidex 9 and Alkathene are both homopolymers, while R2000 is a blend of a low molecular weight polyethylene homopolymer and a high molecular weight copolymer of polyethylene and poly(butene-1). Details of these materials are given in *Table 1*.

The polymers were supplied in granule form and were compression moulded into rectangular plaques. The Rigidex 9 was moulded at 190° C and retained in the press which was then water cooled, the cooling time for the polymer being somewhere between 12 and 50 min. Alkathene was moulded at 180° C, removed from the press and quenched in water. The Rigidex 2000 was compression moulded for us elsewhere and the details are not known. The Rigidex plaques were 20 mm thick and the Alkathene were 10 mm thick.

The material was oriented by hot drawing, using the fol-

* Presented at the Polymer Physics Group (Institute of Physics) Biennial Conference, Shrivenham, September 1977.

† Present address: Rubber and Plastics Research Association, Shawbury, Shrewsbury, Salop, UK.

Table 1 Specification of materials as received

Material and manufacturer	Branches/ 1000 C atoms	M_w	M_N	Density (kg/m ³)
Rigidex 9 (BP Chemicals International Ltd)	<0.3	1.8×10^5	1.0×10^4	966†
Rigidex 2000 (BP Chemicals International Ltd)	<0.3	1.5×10^5 *	1.7×10^4 *	959†
Alkathene WJG 11 (ICI Ltd)	28	3.6×10^5 *	1.5×10^4 *	916†

* Measured by PSCC; † our measurements; remaining data from manufacturer's specifications

lowing procedure. The plaques were machined to a dumb-bell shape with a parallel-sided section 100 mm long and 50 mm wide. The dumb-bells were drawn in a tensile machine with a crosshead speed of 0.17 mm/sec (10 mm/min) at the following temperatures: Rigidex 9 at 70°C; Rigidex 2000 at 75°C; Alkathene at 55°C. After drawing, dumb-bells were held in the machine at constant length and cooled to room temperature in 15 h. They were then removed from the machine and stored at room temperature for at least two days (at least two weeks in the case of Alkathene) before the draw ratio was measured and the material used.

Each of the three materials drew in a characteristic way. Rigidex 9 necked with a load drop and continued to extend beyond the neck with the result that there was a continuous range of draw ratios along the length of the dumb-bell ranging from about 5 just beyond the neck to 25, the highest value used in this work. This value was set, not by the material but by the available travel of the tensile machine crosshead and there is no reason to think that higher draw ratios could not have been obtained with this material. Rigidex 2000 also necked with a load drop, but, unlike Rigidex 9, produced only a narrow range of draw ratio, namely 8 ± 1 . Alkathene did not neck and there was no load drop. The largest draw ratio achieved was 3.5, the limiting factor being the tearing of the sample from points on the surface. Unlike Rigidex 9 and Rigidex 2000, there was considerable shrinkage of the Alkathene in the draw direction at room temperature after removal from the tensile machine (hence the storage period of 2 weeks); the draw ratio was measured after the shrinkage appeared to have ceased.

Samples of the drawn material were annealed in an oil bath over a range of temperatures from the drawing temperature upwards. The samples were unconstrained during annealing. They were then stored for at least 1 week at room temperature before any measurements were made.

X-ray diffraction

Wide- and low-angle X-ray diffraction patterns were recorded on film with the incident beam, which was collimated by means of two pinholes, both parallel and in two directions at right-angles to the draw direction.

Density

Density was measured by weighing in air, and in water with the aid of a sinker; the estimated accuracy was ± 1 kg/m³.

Elastic stiffness constants

The elastic stiffness constants c_{mn} relate the stress com-

ponents σ_m to the strain components ϵ_n according to the generalized Hooke's law.

$$\sigma_m = c_{mn} \epsilon_n$$

Here the suffixes m and n run from 1 to 6 and a repeated suffix (here n) denotes summation. Suffixes 1, 2 and 3 on σ and ϵ denote tensile stress and strain components; 4, 5 and 6 denote shear stress and strain components, the latter being the engineering shear strains. We assumed that the symmetry of the drawn material was orthorhombic and hence that there were nine non-zero components of c_{mn} to be measured, namely c_{11} , c_{22} , c_{33} , c_{44} , c_{55} , c_{66} , c_{12} , c_{23} , c_{13} .

The values of c_{mn} were obtained from measurements of the velocity of propagation of ultrasonic stress wave pulses through the material. The theory of the propagation of plane stress waves through anisotropic materials is discussed in the book by Musgrave¹⁸, and the determination of elastic constants of anisotropic materials by such means has been cited in the Introduction. In the present work the ultrasonic transmitter and receiver were placed in direct contact with the opposite, parallel, faces of the test piece, using a slight smear of oil to ensure good coupling; the time taken for stress wave pulses to travel from transmitter to receiver was measured using a calibrated delay circuit. The travel time was also measured when transmitter and receiver were in direct contact, and the travel time through the sample was taken to be the difference of the two measurements. Both longitudinal and shear wave transducers were used. The frequency was 2.5 MHz with a bandwidth of approximately 1 MHz, and the pulse repetition rate was 1000 sec⁻¹. The wavelength of the stress wave in the test piece was in the range 0.4 to 3.4 mm in these experiments, depending on the velocity of propagation which itself depended on the type of wave propagated and the state of the material. The strain amplitude was estimated to be less than 2×10^{-5} .

Test pieces were cut with pairs of opposite faces perpendicular to the three mutually perpendicular directions which were assumed to be the axes of orthorhombic symmetry, namely, the draw direction, x_3 ; the direction x_2 perpendicular to the face of the plaque; and x_1 , the direction in the plane of the plaque at right angles to the draw direction. In a test piece prepared in this way one true longitudinal wave and two true transverse (shear) waves can be propagated along each of the x_1 , x_2 and x_3 directions. These waves were excited and their velocities V_{mn} measured by placing in turn the longitudinal and the shear wave transducers in contact with each of the three pairs of opposite faces of the test piece. With this geometry, suffixes m and n are equal, their common value being determined by the wave propagation and displacement directions as shown in Table 2. As will be seen from this Table of the nine velocity measurements made only six at most should be different because of equality between associated pairs of shear velocities. These associated pairs were in fact always found to be equal within experimental error. The corresponding six elastic stiffness constants, c_{mn} , were determined from the relationship:

$$c_{mn} = \rho V_{mn}^2 \quad (1)$$

where ρ is the density of the material.

The stiffness constant c_{12} was found by machining a test piece with two opposite faces perpendicular to the direction at 45° to x_1 in the x_1x_2 plane. For this direction of propagation:

$$2\rho V_{S1}^2 = c_{44} + c_{55} \quad (2)$$

$$2\rho V_{S2}^2 = \frac{1}{2}c_{11} + \frac{1}{2}c_{22} + c_{66} - P \quad (3)$$

$$2\rho V_L^2 = \frac{1}{2}c_{11} + \frac{1}{2}c_{22} + c_{66} + P \quad (4)$$

Here

$$P = +[\frac{1}{4}(c_{22} - c_{11})^2 + (c_{12} + c_{66})^2]^{1/2}$$

V_L is the velocity measured with the longitudinal wave transducers, and V_{S1} and V_{S2} are the velocities measured with the shear wave transducers when the displacement in the transmitter is parallel to x_3 in the case of V_{S1} and at right angles to x_3 in the case of V_{S2} . With this geometry the V_{S1} wave in the test piece is a true transverse wave but the V_L and V_{S2} waves in the test piece are not truly longitudinal nor truly transverse. Values of c_{12} were found from equations (3) and (4) and their mean was taken.

The stiffness constants c_{23} and c_{13} were measured in a similar manner by machining appropriate faces on the test piece.

All velocity measurements were made at room temperature.

The attenuation of shear waves in Alkathene was found to be so great that their velocities could not be measured; so for this material only c_{11} , c_{22} and c_{33} were determined.

c_{12} , c_{23} and c_{13} were measured for Rigidex 2000 but showed little or no significant change due to drawing or annealing; for this reason and because of the extra work needed in test piece preparation, these three constants were not measured for Rigidex 9.

Our estimate of the error of the velocity measurements, which includes variation found when the same test piece was measured on separate occasions, is $\pm 0.5\%$. This figure, combined with an error of $\pm 0.1\%$ for the density gives an estimated error of $\pm 1.1\%$ in the values of c_{11} , c_{22} , c_{33} , c_{44} , c_{55} , c_{66}

calculated from equation (1). The error in each of c_{12} , c_{23} and c_{13} is estimated to be $\pm 5\%$, the higher figure being caused by having to make use of values of elastic stiffness constants already determined, as equations (3) and (4) show.

Equations (1) to (4) rest on the assumption that the test piece is of infinite extent. In practice this requires that the transverse dimensions of the test piece should be large compared with the wavelength. Tu, Brennan and Sauer¹⁹ working with circular section test pieces of isotropic metals found experimentally that for their test pieces 'large' in a practical sense meant that the diameter to wavelength ratio, d/λ , needed to be at least 5. As d/λ was reduced below 5, the measured pulse velocity began to decrease. At the same time the pulse became weaker and more distorted, the velocity becoming unmeasurable for d/λ less than about unity. In our experiments the ratio d/λ (where d now denotes the smaller cross-sectional dimension of our rectangular section test piece) was 8.5 or greater in the undrawn material and did not fall below 3.0 for any measurements except those of longitudinal waves in the draw direction, x_3 , in as-drawn Rigidex 9. It would seem, then that the values given for c_{33} in as-drawn Rigidex 9 may have been underestimated; this point is taken up in the discussion section below.

RESULTS

Undrawn material

The undrawn materials were found to be elastically isotropic; the measured elastic constants are included in Tables 3, 4 and 5 for Rigidex 9, Rigidex 2000 and Alkathene, respectively.

Effect of drawing

Drawing produced a texture, as revealed by X-ray diffraction, which was basically similar in all three materials. Wide-angle diffraction (WAXD) patterns showed that the c -axis of the unit cell (the chain axis direction) was oriented in the draw direction, with a - and b -axes randomly oriented around the draw direction. Low-angle X-ray diffraction (LAXD) patterns were of the two point kind, indicating parallel lamellae with surfaces perpendicular to the draw direction.

Table 2 Propagation and displacement directions used to measure c_{mn}

Transducer*	Direction of		c_{mn}
	Propagation	Displacement	
L	x_1	x_1	c_{11}
L	x_2	x_2	c_{22}
L	x_3	x_3	c_{33}
S	x_2	x_3	c_{44}
S	x_3	x_2	c_{44}
S	x_3	x_1	c_{55}
S	x_1	x_3	c_{55}
S	x_1	x_2	c_{66}
S	x_2	x_1	c_{66}

* L denotes longitudinal; S denotes shear

Table 3 Elastic stiffness constants of Rigidex 9. Estimated error, $\pm 1\%$

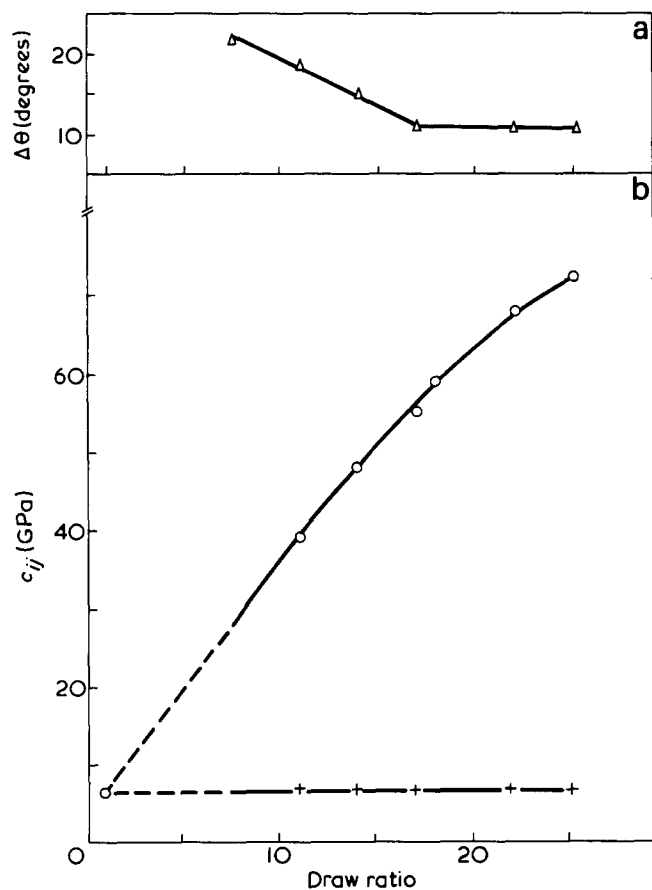
State	c_{11} (GPa)	c_{22} (GPa)	c_{33} (GPa)	c_{44} (GPa)	c_{55} (GPa)	c_{66} (GPa)
Undrawn	6.3	6.3	6.3	1.14	1.14	1.14
Drawn X 11	6.6	6.4	39	—	—	—
Drawn X 18	6.8	6.7	59	1.26	1.29	1.30
Drawn X 18 and annealed at 134°C	7.1	6.9	17.2	1.37	1.29	1.53
Drawn X 25	6.9	6.2	72	—	—	—

Table 4 Elastic stiffness constants of Rigidex 2000. Estimated errors, $\pm 1\%$ in all constants except c_{12} , c_{13} , c_{23} , for which estimated error = $\pm 5\%$

State	c_{11} (GPa)	c_{22} (GPa)	c_{33} (GPa)	c_{44} (GPa)	c_{55} (GPa)	c_{66} (GPa)	$c_{11}-2c_{66}$ (GPa)	c_{12} (GPa)	c_{13} (GPa)	c_{23} (GPa)
Undrawn	5.9	5.9	5.9	1.02	1.02	1.02	3.9	3.9	3.9	3.9
Drawn X 8	5.9	5.7	19.6	0.97	0.98	1.00	3.8	4.0	3.9	3.5
Drawn X 8 and annealed at 130°C	6.3	6.1	8.3	1.04	1.03	1.29	3.7	3.7	4.2	4.0

Table 5 Elastic stiffness constants of Alkathene. Estimated error, $\pm 1\%$

State	c_{11} (GPa)	c_{22} (GPa)	c_{33} (GPa)
Undrawn	3.9	3.9	3.9
Drawn X 2	4.3	4.3	4.8
Drawn X 3.5	4.1	4.2	5.1
Drawn X 3.5 and annealed at 90°C	4.1	4.2	4.3


 Figure 1 Rigidex 9 drawn at 70°C. (a) (200) arc width $\Delta\theta$ (Δ), and (b) elastic stiffness constants c_{11} (+) and c_{33} (\circ), plotted against draw ratio

Variations in this basic texture caused by increasing the draw ratio were investigated in Rigidex 9 over a range of draw ratios from 7.5 to 25 and in Alkathene over a range from 2 to 3.5. Rigidex 2000 yielded only a draw ratio of 8; its texture was similar to that of Rigidex 9 at the same draw ratio.

In Rigidex 9 it was found that a high degree of c -axis orientation had already been established at a draw ratio of 7.5, as judged by the WAXD arc widths. The arc width of the (200) reflection is plotted against draw ratio in Figure 1; a small decrease in arc width occurred up to a draw ratio 18 and thereafter there was no detectable change. (In this as in all Figures in this paper, the curves are drawn simply to link the plotted points and do not represent theoretical relationships). The two spots in the LAXD pattern spread along layer lines at right-angles to the draw direction with increasing ratio but the long spacing, as measured between the centres of the spots, remained unchanged at 22.6 ± 0.6 nm. There was a void streak through the centre of the pattern elongated in the direction at right angles to the draw direc-

tion and this elongation increased with drawing. No change in density with drawing was detected by measurement, although there were other indications of voiding.

The measurements on drawn Alkathene covered a range of draw ratio from 2 to 3.5. The degree of orientation of the chain axis was much lower than was the case in Rigidex 9 but, as Figure 2 shows, the rate of decrease of WAXD (200) arc width was substantially greater, and was approximately constant over the range studied. The LAXD patterns were like those obtained from Rigidex 9, except for an increase in long spacing from 11.2 ± 0.3 nm at a draw ratio of 2 to 13.1 ± 0.3 nm at a draw ratio of 3.5.

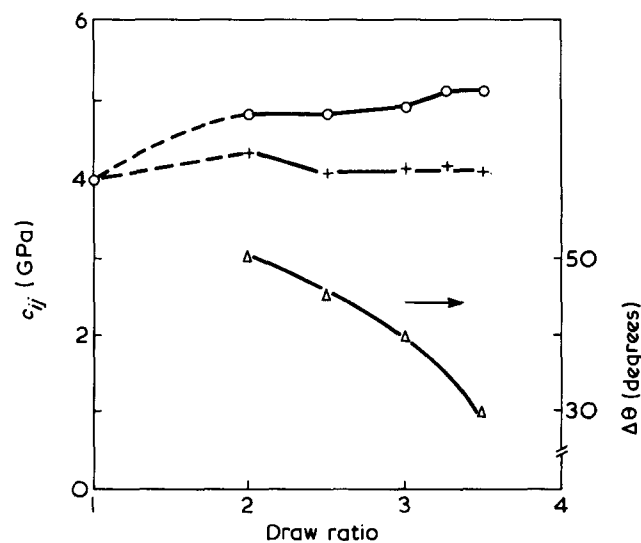
Some representative elastic constant measurements for Rigidex 9, Rigidex 2000 and Alkathene after drawing are included in Tables 3, 4 and 5, respectively.

The stiffness constants c_{11} and c_{33} are plotted against draw ratio for Rigidex 9 in Figure 1 and for Alkathene in Figure 2; (the lines are broken on the left-hand side of the graphs to indicate the region within which the drawn texture described above was set up).

Effect of annealing the drawn material

Rigidex 9 samples of draw ratio 18, Rigidex 2000 samples of draw ratio 8 and Alkathene samples of draw ratio 3.5 were annealed at temperatures from the draw temperature upwards and were allowed to shrink freely in the draw direction. The annealing treatment did not change the basic texture from that of the drawn state, although there was some disorienting of the chain axis. Figures 3, 4 and 5 show the length contraction in the draw direction and the change in WAXD (200) arc width with increasing annealing temperature for Rigidex 9, Rigidex 2000 and Alkathene. At the lower end of the annealing range the LAXD spots contracted along the layer lines became better defined with increasing annealing temperature, but at higher temperatures the spots increased in size in all directions. The void streak disappeared, and the density increased by about 10%. Throughout the annealing range the long spacing, determined from the distance between the centres of the two spots in the LAXD pattern, increased in the usual characteristic manner.

Values of the stiffness constants measured on samples annealed at the upper end of the temperature range are in-


 Figure 2 Alkathene drawn at 55°C. (200) arc width $\Delta\theta$ (Δ), and elastic stiffness constants c_{11} (+) and c_{33} (\circ), plotted against draw ratio

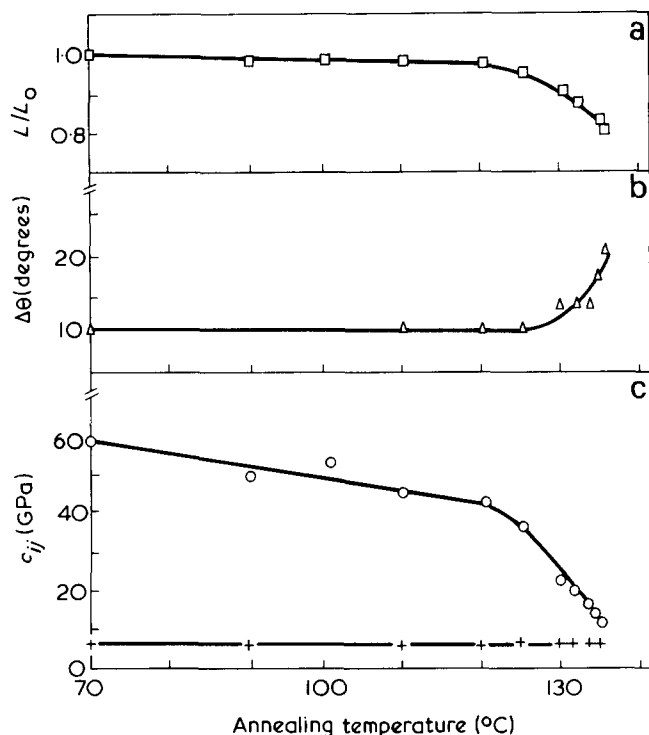


Figure 3 The annealing of Rigidex 9 drawn $\times 18$ at 70°C . (a) L/L_0 , the ratio annealed length/drawn length in the draw direction (\square); (b) the (200) arc width $\Delta\theta$ (Δ), and (c) the elastic stiffness constants c_{11} (+) and c_{33} (\circ), plotted against the annealing temperature

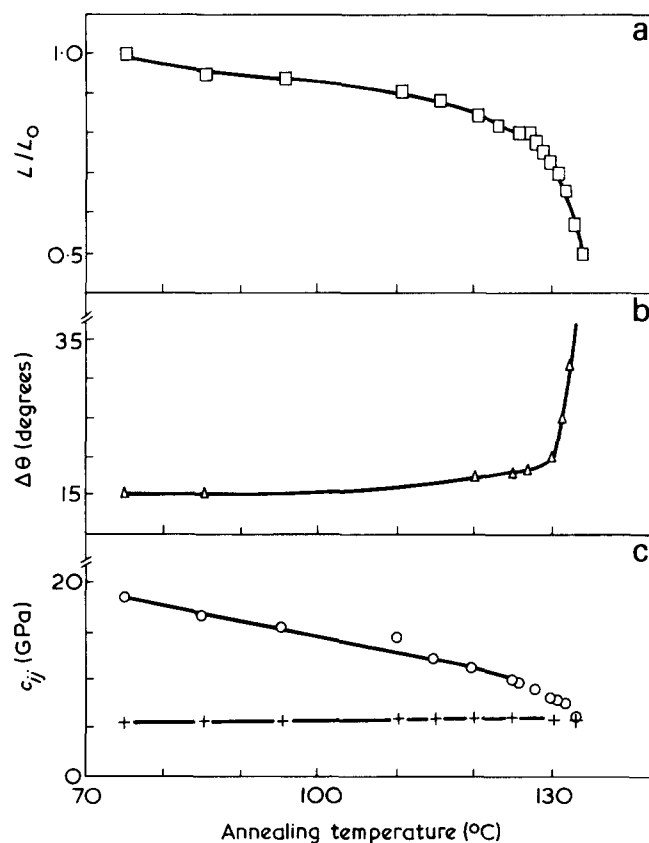


Figure 4 The annealing of Rigidex 2000 drawn $\times 8$ at 75°C . (a) L/L_0 , the ratio annealed length/drawn length in the draw direction (\square); (b) the (200) arc width $\Delta\theta$ (Δ), and (c) the elastic stiffness constants c_{11} (+) and c_{33} (\circ), plotted against the annealing temperature

cluded in Tables 3, 4 and 5. Plots of c_{11} and c_{33} against annealing temperature for Rigidex 9, Rigidex 2000 and Alkathene are included in Figures 3, 4 and 5, respectively.

Increased drawing, which increased the length of the sample in the draw direction, reduced the WAXD (200) arc width and increased c_{33} , whereas annealing produced the reverse effects. However the relationship between length and c_{33} was not reversible, as is illustrated in Figure 6 for Rigidex 9 and Figure 7 for Alkathene, in which c_{33} is plotted against the length of the sample in the draw direction relative to the undrawn length. In both materials the change in c_{33} accompanying a given length change was much greater on annealing than on drawing.

The variations in the stiffness constants c_{11} , c_{22} , c_{44} , c_{55} and c_{66} of Rigidex 9 and Rigidex 2000 are shown on an expanded scale as a function of annealing temperature in Figures 8 (c_{11} , c_{22} , the transverse longitudinal stiffnesses) and 9 (c_{44} , c_{55} , c_{66} , the shear stiffnesses). The stiffness constants c_{11} and c_{22} were nearly equal as were c_{44} and c_{55} ; separate curves have been drawn where it is thought that the differences between the members of a pair were greater than the experimental error. In both materials c_{11} , the longitudinal stiffness constant in the direction perpendicular to the plane of the plaque, was consistently greater than c_{22} ; annealing caused a small increase. The shear stiffness constants c_{44} , c_{55} and c_{66} were approximately equal to one another after drawing, and all increased with annealing temperature at the lower end of the annealing range. At the upper end, c_{66} continued to rise while c_{44} and c_{55} fell; this divergence shows more clearly in the case of Rigidex 2000.

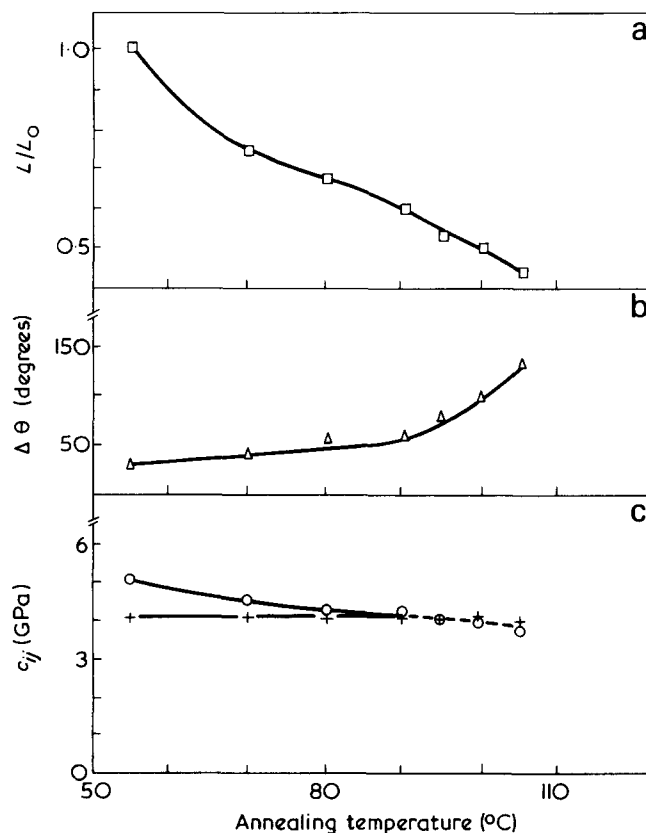


Figure 5 The annealing of Alkathene drawn $\times 3.5$ at 55°C . (a) L/L_0 , the ratio annealed length/drawn length in the draw direction (\square); (b) the (200) arc width $\Delta\theta$ (Δ) and (c) the elastic stiffness constants c_{11} (+) and c_{33} (\circ), plotted against the annealing temperature

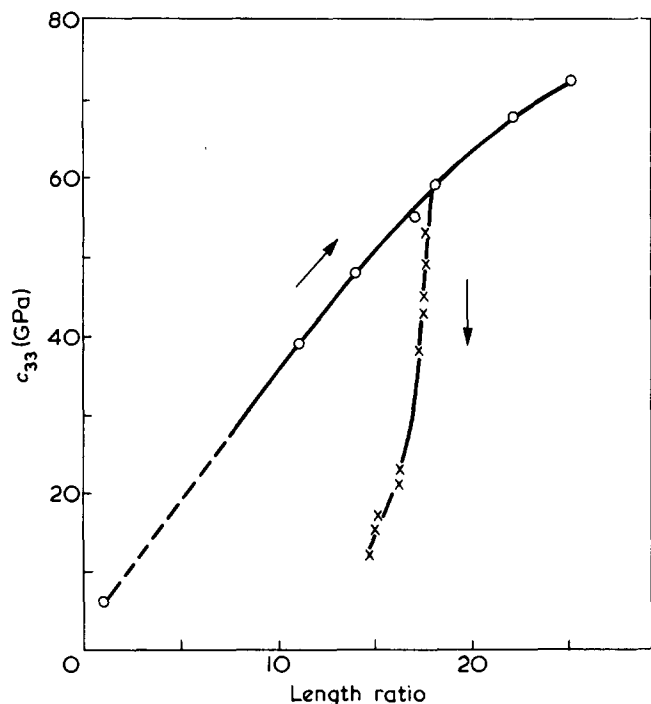


Figure 6 Rigidex 9, c_{33} plotted against the ratio of length in the draw direction to undrawn length, for drawing (○) and annealing (X)

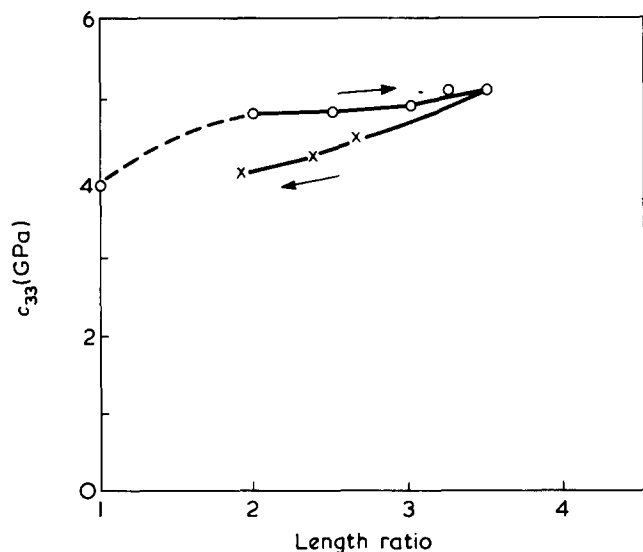


Figure 7 Alkathene, c_{33} plotted against the ratio of length in the draw direction to undrawn length, for drawing (○), and annealing (X)

DISCUSSION

Our measured values of c_{11} and c_{66} for the unoriented material are in good agreement with those of other workers using a similar technique in the MHz range⁹⁻¹¹, as is shown in Table 6. There is a clear dependence on density in the case of c_{11} ; there does not seem to be a noticeable frequency dependence in the range covered, 0.5 to 4.3 MHz. The increase in c_{11} with density can be ascribed to an increase in crystallinity.

Measurements on oriented Rigidex 2000 both in the drawn state and after annealing showed that this material was transversely isotropic elastically. The conditions for transverse isotropy are $c_{11} = c_{22}$; $c_{12} = c_{11} - 2c_{66}$; $c_{13} = c_{23}$ and $c_{44} = c_{55}$. Table 4 shows that these conditions were met. The data

for Rigidex 9 are not so complete, as c_{12} , c_{13} and c_{23} were not measured, but c_{11} and c_{22} were approximately equal, and so were c_{44} and c_{55} . In Alkathene only c_{11} and c_{22} could be compared, and these were equal.

We have not found in the literature any values of the stiffness constants of oriented polyethylene determined in the MHz range with which to compare our own. 'Static' (1 min moduli) or torsion pendulum methods have been used to determine all five compliance constants of transversely oriented polyethylene fibres at room temperature¹⁶, and to deter-

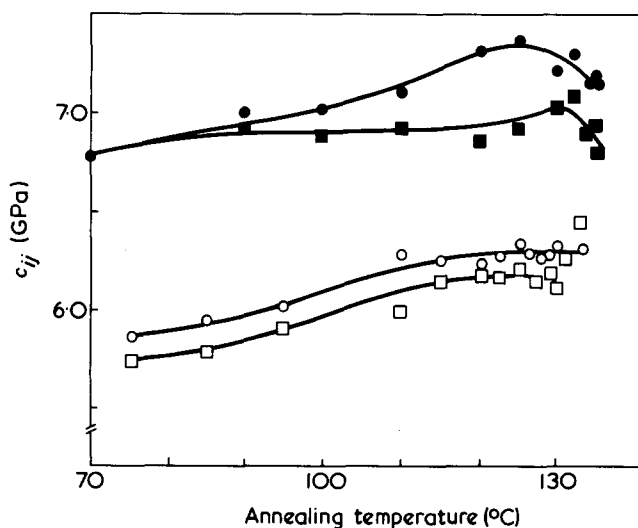


Figure 8 c_{11} and c_{22} plotted against annealing temperature. Rigidex 9 drawn at 70°C: c_{11} (●), c_{22} (■); Rigidex 2000 drawn at 75°C: c_{11} (○), c_{22} (□)

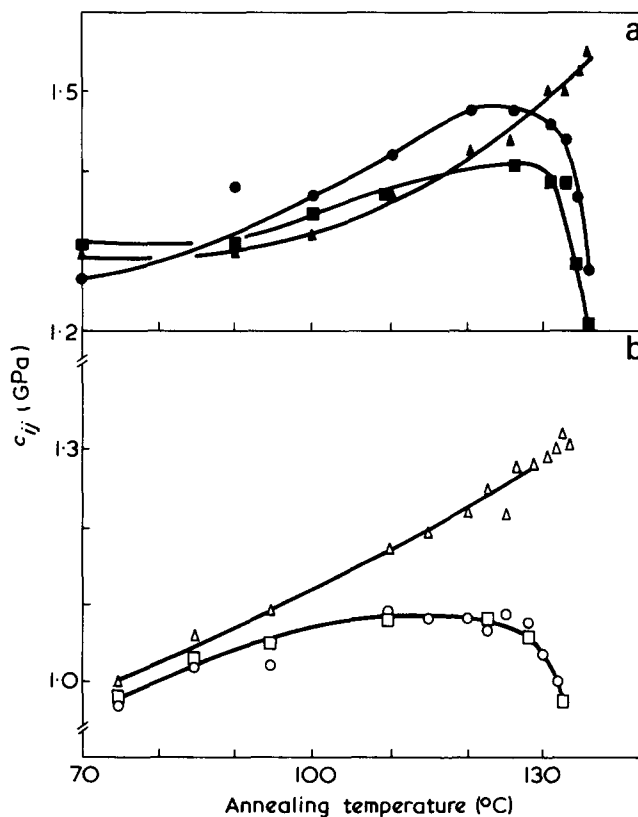


Figure 9 c_{44} , c_{55} and c_{66} plotted against annealing temperature. Rigidex 9 drawn at 70°C: c_{44} (●), c_{55} (■), c_{66} (▲); Rigidex 2000 drawn at 75°C: c_{44} (○), c_{55} (□), c_{66} (△)

mine some of the compliance constants of oriented polyethylene sheet in the range -180° to -70°C (ref 17). Values from these two references are given in *Table 7*, together with compliance constants calculated from the stiffness constants we measured for as-drawn Rigidex 2000. The very large differences between our compliance constants and those of ref 16 (a ratio of about 1:5 in the case of s_{11}) may be partly due to structural differences between sheet and fibre (although s_{11} and s_{22} in particular are unlikely to be structure sensitive); partly due to differences in the magnitude of the strains employed and partly due to the difference in frequency, which was about seven decades, a difference large compared with the spread in *Table 6*, where no frequency effect is apparent. (If the significant factor is strain rate rather than frequency the difference is not so large, as ultrasonic strains are significantly smaller than those employed in the usual 'static' or low frequency measurements which partly compensates for the higher frequency.)

A comparison of ultrasonic (4 MHz) and 'static' (30 sec, maximum strain 5×10^{-3}) measurements of s_{11} and s_{33} have been made¹² at a temperature of 25°C using the same samples of PMMA and polystyrene, both unoriented and oriented. The ratio of ultrasonic to static compliance values was about 2:1 in PMMA and about 1.3:1 in polystyrene. If this is a frequency effect then, thinking in terms of time-temperature superposition, it may be relevant to note that a 2:1 reduction in the s_{11} compliance of PMMA measured at a strain rate of 10^{-4} sec^{-1} can be obtained by reducing the measuring temperature from 25° to $\sim -85^{\circ}\text{C}$ (ref 20): that is to say, the ultrasonic compliance of PMMA at 25°C is about equal to the 'static' compliance at -85°C . It may be significant that our compliance constants are quite close to the -70°C values given in *Table 7* (read from the graph in *Figure 5* of ref 7) which were measured at 10 sec at a strain not exceeding 1×10^{-3} , on polyethylene sheet, biaxially drawn ($\times 9$) at 120°C .

Table 6 c_{11} and c_{66} , unoriented polyethylene

Density (kg/m ³)	Frequency (MHz)	c_{11} (GPa)	c_{66} (GPa)	Reference
916	4.3	3.8	—	9
916	2.5	3.9	—	This paper
920	0.5	4.2	—	11
950	0.5	5.7	—	11
959	2.5	5.9	1.02	This paper
964	3.0	6.4	—	9
966	2.5	6.2	1.15	This paper
967	1.0	—	1.26	10
967	3.0	—	1.32	10

The velocities from refs 9, 10 and 11 were brought to 20°C using a temperature coefficient of $7\text{ m/sec}^{\circ}\text{C}$ from refs 9 and 10; c_{11} and c_{66} were then calculated

Table 7 Elastic compliance constants of high density polyethylene from ref 16 and 17, and calculated from the stiffness constants of as-drawn Rigidex 2000 (*Table 4*)

Temperature ($^{\circ}\text{C}$)	s_{11} (GPa) ⁻¹	s_{33} (GPa) ⁻¹	s_{44} (GPa) ⁻¹	s_{66} (GPa) ⁻¹	s_{12} (GPa) ⁻¹	s_{13} (GPa) ⁻¹	$s_{44} + 2s_{23}$ (GPa) ⁻¹	Reference
~ 20	1.5	0.23	1.7	6.2	-1.6	-0.08	1.5	16
-70	0.25	0.07	—	—	—	—	0.75	17
-180	0.15	0.03	—	—	—	—	0.5	17
~ 20	0.31	0.06	1.0	1.0	-0.19	-0.023	0.95	This paper

This material had a texture similar to our own except that the a and b crystal axes were also oriented.

An apparent frequency effect in the tensile modulus of high modulus polyethylene fibres has been reported²¹, the modulus approximately doubling with an increase in frequency from 10 sec^{-1} to $7 \times 10^3\text{ sec}^{-1}$. Values of tensile modulus in the draw direction of high modulus hot-drawn polyethylene sheet have been published by several authors^{2,7,22}. Some of these values are given in *Table 8*, together with data calculated from our measurements of the stiffness constants of Rigidex 9 (modulus values were read from graphs in ref 2 and 22 and draw ratios as near as possible to those used on Rigidex 9 were selected). It is difficult to disentangle the various effects of the measurement parameters of frequency and strain amplitude on the one hand and sample preparation on the other. Referring to *Table 8*, a comparison of the room temperature measurements from refs 2 and 22 suggests quite a pronounced frequency effect, and comparison of refs 7 and 22 gives an indication of variations due to sample preparation. Ref 2 shows the effect of measurement temperature, and data in ref 22, not quoted here, shows a pronounced effect due to changing the measurement strain. The quite close agreement between our Rigidex 9 values and those of ref 2 measured at 20°C may, therefore, be fortuitous and not only because of the factors just discussed. As stated in the Experimental section above, our values of c_{33} may have been underestimated due to the ratio d/λ being too small. We have not been able to estimate theoretically the magnitude of this effect but as the received pulses were strong we think the error may be small¹⁹ and we plan to make measurements to clear up this point. There is, however, no doubt that our drawn Rigidex 9 was in the high modulus class.

Irrespective of the absolute values of the measured stiffness constants reported here, some clear features have emerged regarding the way in which the constants were or were not affected by drawing and by subsequent annealing.

The stiffness constant most affected by drawing was c_{33} ; by comparison the effect on the other constants was small. This parallels the behaviour found in PMMA¹² polystyrene¹² and PVC¹³. Similarly c_{33} was the most affected by subsequent annealing.

The increase in c_{33} correlated with draw ratio for all three materials, as other authors have reported for tensile modulus, in the sense that the higher the draw ratio the higher the value of c_{33} .

The decrease in c_{33} on annealing did not relate to length change in the same way as the increase in c_{33} on drawing.

The changes in c_{33} on drawing and annealing did not correlate with changes in crystalline orientation. Once the crystal texture of the drawn structure was set up there was little change in the degree of orientation in Rigidex 9 with further drawing but a large increase in c_{33} , while in Alkathene there was a significant increase in the degree of orientation accom-

Table 8 Comparison of tensile modulus (s_{33}^{-1}) values of drawn polyethylene measured in the draw direction

Reference	Material	Frequency or time of measurement	Strain	Temperature	Draw ratio	s_{33}^{-1} (GPa)
22	Rigidex 50	10 sec	1×10^{-3}	Room	11	10
					19	31
					25	45
2	Rigidex 50	20 Hz	$\pm 1 \times 10^{-3}$	20°C	11	31
					19	53
					25	72
2	Rigidex 50	20 Hz	$\pm 1 \times 10^{-3}$	-70°C	11	44
					19	70
					25	93
7	Rigidex 50	10 sec	1×10^{-3}	Room	11	7
					18	24
					25	58
This paper	Rigidex 9	2.5 MHz	$< \pm 2 \times 10^{-5}$	Room	11	36
					18	56
					25	69

panied by only a small increase in c_{33} . On annealing Rigidex 9 and Rigidex 2000, c_{33} decreased markedly with little change in the degree of orientation, whereas in Alkathene the decrease in c_{33} was small while the degree of orientation decreased significantly.

That the degree of crystalline orientation remains unchanged beyond a draw ratio of ~ 5 while draw ratio and tensile modulus in the draw direction both increase has been remarked on by a number of workers^{2,23,24}. Various models of the drawn state have been discussed. All have in common that the tensile modulus in the draw direction falls below the theoretical crystal modulus because of the presence of an amorphous phase of lower stiffness through which the load is transmitted. In some cases the model used is of a somewhat formalized kind expressed in terms of a series or series-parallel coupling of crystalline and amorphous phases^{1,2,17,23} (here the terms series and parallel are relative to the draw direction). More structurally descriptive models have been discussed in terms of fibrils and microfibrils^{3,4} or of fibre reinforced materials^{8,25}. Glenz and Peterlin²⁴ used infra-red measurements to show that the crystalline phase became fully oriented in the early stages of drawing (at a draw ratio of about 5) while the degree of orientation of the amorphous phase continued to increase as drawing continued. On annealing, the amorphous phase began to disorient and the sample to contract as soon as the annealing temperature exceeded the drawing temperature, while the crystalline orientation was unaffected until a significantly higher temperature was reached. Furthermore, the measured orientation function showed qualitatively the same kind of hysteresis relative to sample length changes as we found for c_{33} . Our measurements of c_{33} qualitatively fit well into Glenz and Peterlin's picture. Smith, Davies, Capaccio and Ward², using an n.m.r. technique, also found evidence for the orienting of the amorphous phase on drawing at a stage when the crystalline phase was already oriented, but considered that the increase in tensile modulus was due not to the orienting of the amorphous phase but to a decrease in its volume fraction. Arridge, Barham and Keller²⁵ and Barham and Arridge⁸, using a fibre composite model, attributed the increase in tensile modulus to a change in the aspect ratio of reinforcing crystal fibres. Our results do not appear to differentiate between these models, although one point can be made. In the fibre composite model^{8,25} the tensile modulus depends not only on the aspect ratio of the crystal fibre but also on

the shear modulus of the surrounding matrix. In view of the comparatively small changes we found in shear stiffness constants c_{44} and c_{55} during drawing and annealing it would seem that the change we observed in c_{33} could not be ascribed to changes in the matrix shear modulus.

We now turn to the stiffness constants c_{11} , c_{22} , c_{44} and c_{66} and consider them in the light of a simple series model^{17,26}. In such a model²⁶:

$$c_{11} = \nu^c c_{11}^c + \nu^a c_{11}^a \quad (5)$$

approximately, where ν denotes volume fraction and superscripts c and a refer to the crystalline and amorphous phases, respectively. As a first approximation we neglect the term $\nu^a c_{11}^a$ as being small in comparison with $\nu^c c_{11}^c$, obtaining

$$c_{11} = \nu^c c_{11}^c \quad (6)$$

A similar expression holds for c_{22} . Odajima and Maeda²⁷ have calculated two sets of theoretical values for c_{11}^c and c_{22}^c which differ one from the other by 30 and 60%. The near equality of the measured values of c_{11} and c_{22} is explained by the observed random orientation of the a and b crystal axes about the draw direction. It would be of interest to measure c_{11} and c_{22} of samples in which the a and b axes are also oriented. The near constancy of c_{11} and c_{22} with drawing and annealing are consistent with the near constancy observed in the degree of crystal orientation. The small increases in c_{11} and c_{22} during annealing (about 10%) could be due to void closure or to an increase in crystallinity (ν_c) or both (an increase of 10% in density was measured). When ν_c is calculated from the density and inserted in equation (6) together with the measured value of c_{11} averaged with c_{22} , the following values for $\langle c_{11}^c \rangle$, the average of c_{11}^c and c_{22}^c , are obtained: 7.5 GPa from the Alkathene data; 7.5 GPa from the Rigidex 2000 data and 8.0 GPa from the Rigidex 9 data. These values are close to the two theoretical estimates of $\langle c_{11}^c \rangle$ made by Odajima and Maeda²⁷, 6.7 GPa and 7.8 GPa. If these values of $\langle c_{11}^c \rangle$ are inserted in equation (5) we obtain for c_{11}^a , 2.6 GPa and -0.9 GPa, showing that a good estimate of c_{11}^a cannot be obtained.

As regards the shear stiffness constants, the series model gives the following expressions for c_{44} and c_{66} , based on the assumptions that for 44 shear (parallel to and across the draw direction) the shear stress is the same in both phases, while

in 66 shear (at right angles to the draw direction) the shear strain is the same in both phases^{17,26}:

$$c_{44} = (v^c/c_{44}^c + v^a/c_{44}^a)^{-1} \quad (7)$$

$$c_{66} = v^c c_{66}^c + v^a c_{66}^a \quad (8)$$

Odajima and Maeda's two estimates for the average of c_{44} and c_{55} are 1.8 GPa and 1.9 GPa and the use of either value in (7) gives a positive result for c_{44}^a , namely 0.4 GPa, indicating that the contributions of crystalline and amorphous phases to c_{44} are approximately equal. Equation (8) is of the same form as equation (5) and leads to the conclusion that c_{66} , like c_{11} , is dominated by the crystalline phase and an estimate of c_{66}^a is not possible. There is no reason here for the observed equality of c_{44} and c_{66} over most of the range covered by the measurements, and this equality must be regarded, in terms of the model, as fortuitous and not explained.

In conclusion, the ultrasonic contact probe method of measuring stiffness constants has been found to be quick, and it is satisfactory provided the transverse dimensions of the test piece are large enough. More work is to be done to establish how large is large. Our results are in agreement with those of other workers in finding that the stiffness in the draw direction can increase markedly with increasing draw ratio without much change in the crystalline texture. We have found that by comparison the other elastic stiffness constants are little changed. A comparison of numerical values with other workers has shown differences presumed to arise from differences in the parameters of the various measurement techniques and in material preparation but the relative importance of the various factors is not yet clear.

ACKNOWLEDGEMENTS

The ultrasonic velocity measurements were made at the National Physical Laboratory, Teddington, with the kind permission of the Director. The authors are also indebted to Mr M. F. Markham for advice and help when using the appa-

ratus, but they take full responsibility for the actual measurements. Dr Watkinson was in receipt of a Science Research Council studentship when the work was carried out.

REFERENCES

- 1 Hadley, D. W. and Ward, I. M. *Rep. Prog. Phys.* 1975, **38**, 1143
- 2 Smith, J. B., Davies, G. R., Capaccio, G. and Ward, I. M. *J. Polym. Sci. (Polym. Phys. Edn)* 1975, **13**, 2331
- 3 Peterlin, A. *Adv. Chem. Series* 1975, **142**, 1
- 4 Peterlin, A. *Kolloid Z.* 1975, **253**, 809
- 5 McRae, M. A., Maddams, W. F. and Preedy, J. E. *J. Mater. Sci.* 1976, **11**, 2036
- 6 Britton, R. N., Jakeways, R. and Ward, I. M. *J. Mater. Sci.* 1976, **11**, 2053
- 7 Barham, P. J. and Keller, A. *J. Mater. Sci.* 1976, **11**, 27
- 8 Barham, P. J. and Arridge, R. G. C. *J. Polym. Sci. (Polym. Phys. Edn)* 1977, **15**, 1177
- 9 Arnold, N. D. and Guenther, A. H. *J. Appl. Polym. Sci.* 1966, **10**, 731
- 10 Asay, J. R. and Guenther, A. H. *J. Appl. Polym. Sci.* 1967, **11**, 1087
- 11 Folds, D. C. *J. Acoust. Soc. Am.* 1972, **52**, 426
- 12 Wright, H., Faraday, C. S. N., White, E. F. T. and Treloar, L. R. G. *J. Phys. (D)* 1971, **4**, 2002
- 13 Rawson, F. F. and Rider, J. G. *J. Phys. (D)* 1974, **7**, 41
- 14 Markham, M. F. *Composites* 1970, **1**, 145
- 15 Smith, R. E. *J. Appl. Phys.* 1972, **43**, 2555
- 16 Hadley, D. W., Pinnock, P. R. and Ward, I. M. *J. Mater. Sci.* 1969, **4**, 152
- 17 Buckley, C. P. *J. Mater. Sci.* 1974, **9**, 100
- 18 Musgrave, M. J. P. 'Crystal Acoustics', Holden-Day, San Francisco-Cambridge-London-Amsterdam, 1970
- 19 Tu, L. Y., Brennan, J. N. and Sauer, J. A. *J. Acoust. Soc. Am.* 1955, **27**, 550
- 20 ICI Technical Service Note PX 122, 'Perspex Acrylic sheet', 3rd Edn, Sheet Group, ICI Plastics Division, Welwyn Garden City, Herts, UK
- 21 Capiati, N. J. and Porter, R. S. *J. Polym. Sci. (Polym. Phys. Edn)* 1975, **13**, 1177
- 22 Capaccio, G. and Ward, I. M. *Polymer* 1974, **15**, 233
- 23 Smith, J. B., Emanuel, A. J. and Ward, I. M. *Polymer* 1975, **16**, 57
- 24 Glenz, W. and Peterlin, A. *J. Polym. Sci. (A-2)* 1971, **9**, 1191
- 25 Arridge, R. G. C., Barham, P. J. and Keller, A. *J. Polym. Sci. (Polym. Phys. Edn)* 1977, 389
- 26 Watkinson, K. M. *PhD Thesis* University of Surrey (1977)
- 27 Odajima, A. and Maeda, T. *J. Polym. Sci. (C)* 1966, **15**, 55